Figures and figure supplements

Arginase 1 is a key driver of immune suppression in pancreatic cancer

Rosa E Menjivar *et al*.

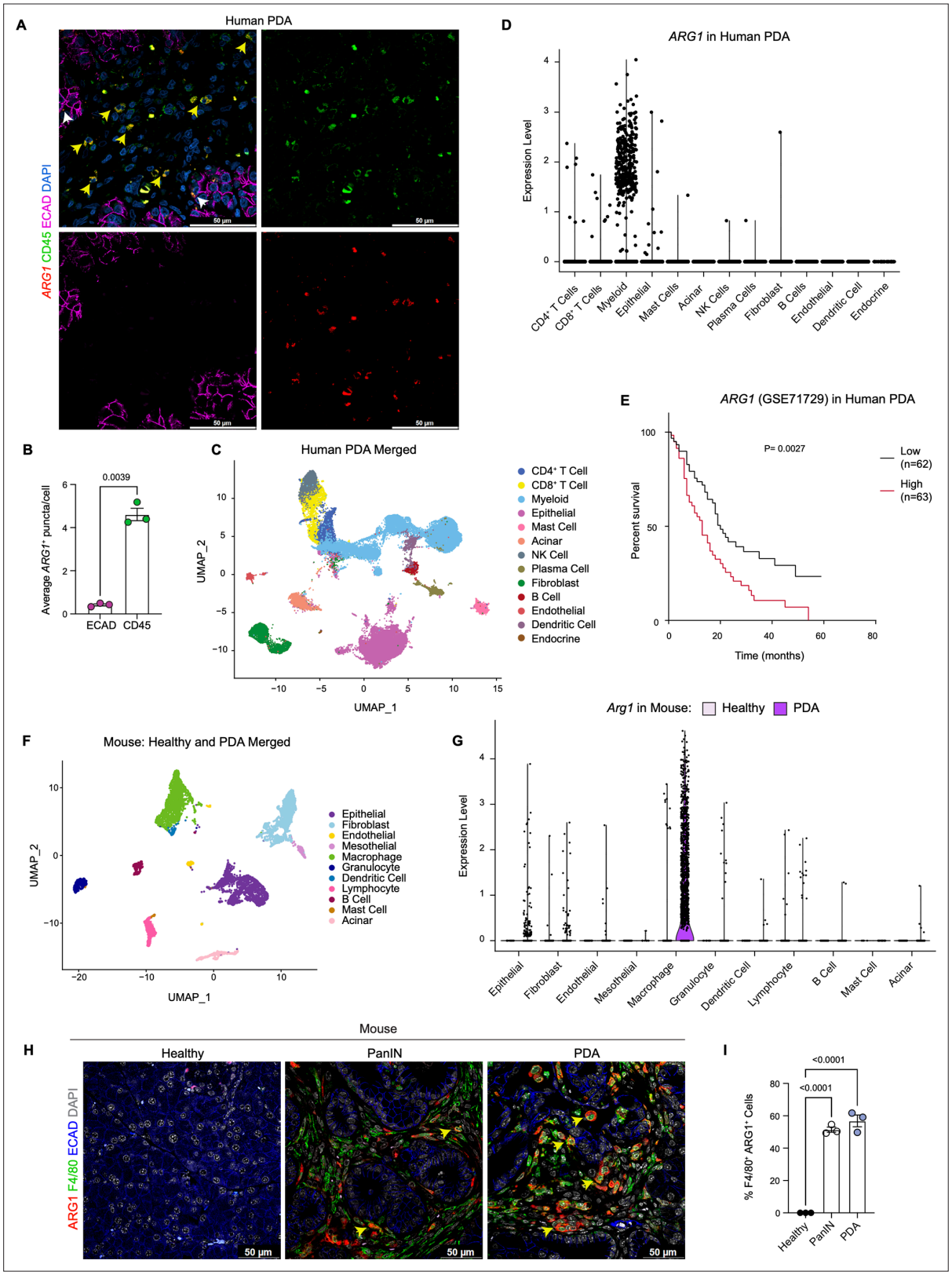

Figure 1. Arginase 1 (Arg1) is highly expressed in human and mouse myeloid cells. (**A**) Representative image of RNA in situ hybridization (ISH) of *ARG1* (red) and co-immunofluorescence staining of immune (CD45, green) and epithelial (E-cadherin [ECAD], magenta) cells in human pancreatic ductal adenocarcinoma (PDA). Counterstain, DAPI (blue). White arrows point to *ARG1*-ISH in ECAD$^+$ cells, and yellow arrows point to *ARG1*-ISH in CD45$^+$ cells. Scale bar, 50 µm. (**B**) Quantification of average *ARG1*$^+$ puncta in CK19 and CD45 cells. Unpaired t test with Welch's correction was used to determine

Figure 1 continued on next page

Figure 1 continued

statistical significance. (**C**) Uniform manifold approximation and projection (UMAP) visualization of 13 identified cell populations from single-cell RNA sequencing (sc-RNA-seq) of 16 human PDA tumors. Data from ***Steele et al., 2020***. (**D**) Violin plot of normalized gene expression of *ARG1* in the identified cell populations from the human PDA sc-RNA-seq. (**E**) Survival analysis of a human PDA microarray data set (GSE71729) with low (n=62) and high (n=63) *ARG1* expression. Statistical significance was determined using the Kaplan Meier overall survival Logrank test. (**F**) UMAP visualization of 11 identified populations from healthy and PDA merged mouse sc-RNA-seq. (**G**) Violin plot of normalized gene expression of *Arg1* in the identified cell populations from mouse sc-RNA-seq. (**H**) Representative co-immunofluorescence staining for ARG1 (red), macrophages (F4/80, green), and epithelial (ECAD, blue) cells in mouse tissue at different stages of disease. Counterstain, DAPI (gray). Scale bar, 50 μm. Yellow arrows indicate ARG1 expression in $F4/80^+$ cells. (**I**) Quantification of $F4/80^+$ $ARG1^+$ cells in healthy, PanIN, and PDA mouse tissue. Statistical significance was determined using an ordinary one-way ANOVA with multiple comparisons. p Value was considered statistically significant when $p<0.05$.

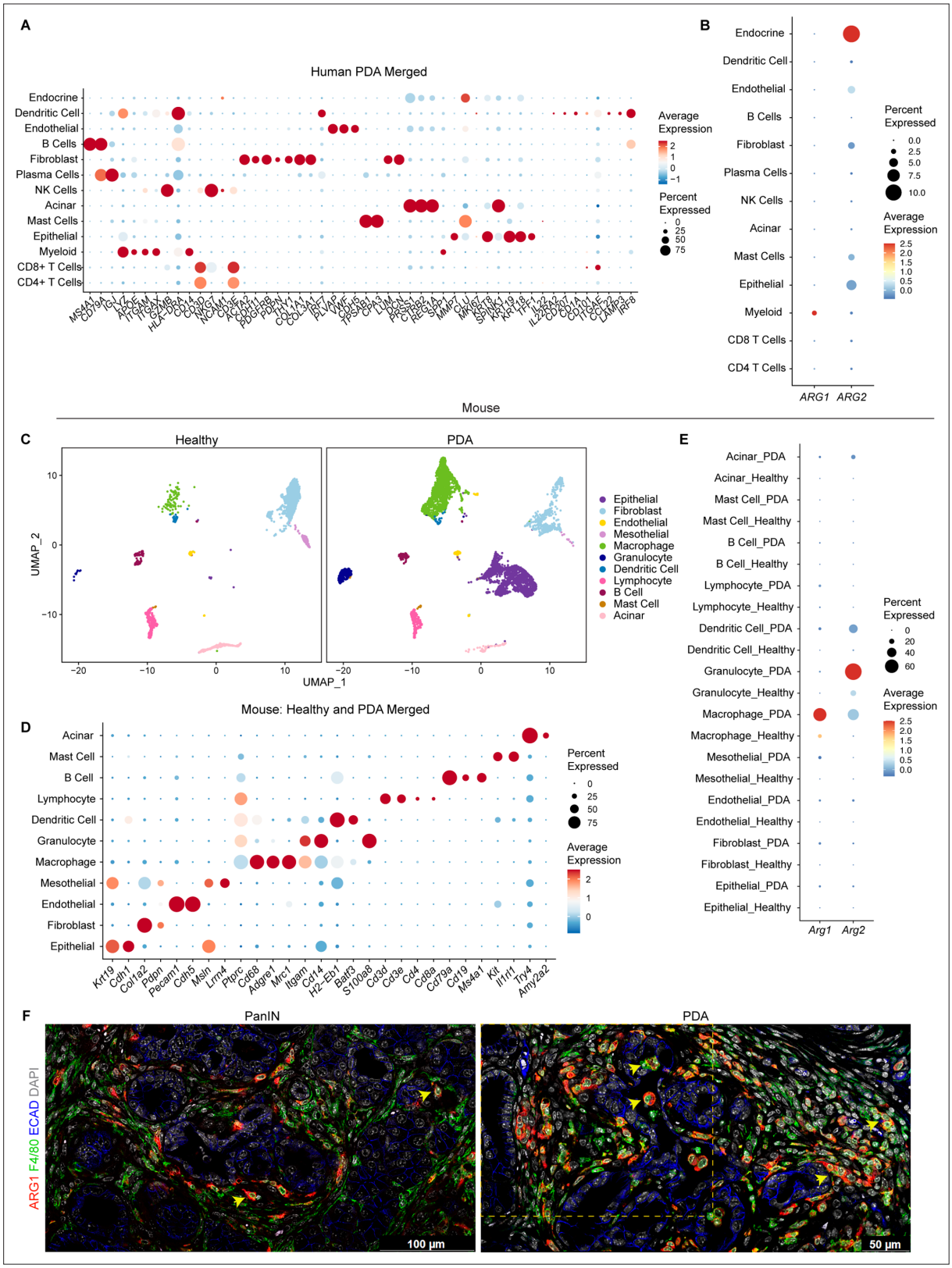

Figure 1—figure supplement 1. Arginase 1 (Arg1) expression in human and mouse myeloid cells. (**A**) Dot plot showing the lineage markers used to identify the different cell populations in the human single-cell RNA sequencing (sc-RNA-seq). Dot color indicates average expression and dot size indicates expression frequency. (**B**) Dot plot showing normalized gene expression levels of *ARG1 and ARG2* in the human sc-RNA-seq. (**C**) Uniform manifold approximation and projection (UMAP) visualizations comparing defined cell populations in healthy and pancreatic ductal adenocarcinoma

Figure 1—figure supplement 1 continued on next page

Figure 1—figure supplement 1 continued

(PDA) mouse sc-RNA-seq. (**D**) Dot plot showing the lineage markers used to identify the distinct cell populations in healthy and PDA mouse sc-RNA-seq. (**E**) Dot plot showing normalized gene expression levels of *Arg1* and *Arg2* in healthy and PDA mouse sc-RNA-seq. (**F**) Representative co-immunofluorescence staining for ARG1 (red), macrophages (F4/80, green), and epithelial (E-cadherin [ECAD], blue) cells in mouse tissue during PanIN and PDA stages of disease. Quantification of $F4/80^{+}$ $ARG1^{+}$ cells is shown in ***Figure 1I***. Yellow dotted box marks the area shown in main ***Figure 1H***. Scale bar for PanIN image is 100 μm; for PDA is 50 μm.

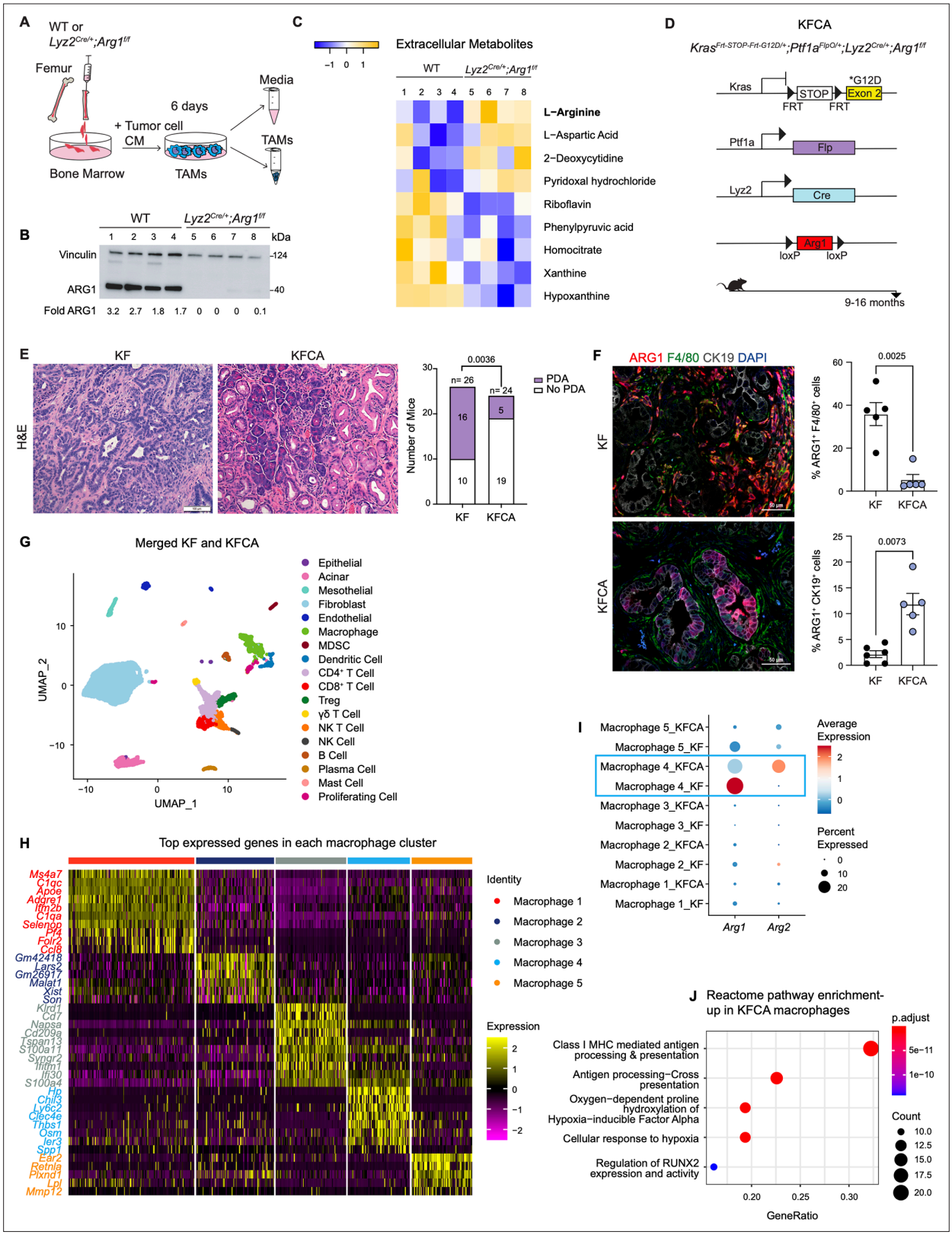

Figure 2. Arginase 1 (*Arg1*) deletion in myeloid cells reduces tumor progression and induces macrophage repolarization in a spontaneous pancreatic ductal adenocarcinoma (PDA) mouse model. (**A**) Schematic illustration for the generation of tumor-associated macrophages (TAMs) from wild-type (WT) and *Lyz2*$^{Cre/+}$;*Arg1*$^{f/f}$ mice. (**B**) Representative image of western blot for ARG1 levels in WT and *Lyz2*$^{Cre/+}$;*Arg1*$^{f/f}$ TAMs. Vinculin, loading control. (**C**) Heatmap of statistically significantly different extracellular metabolites from WT (lanes 1–4) and *Lyz2*$^{Cre/+}$;*Arg1*$^{f/f}$ (lanes 5–8) TAM media. (**D**) Genetic

Figure 2 continued on next page

Figure 2 continued

makeup of the *Kras*$^{Frt\text{-}STOP\text{-}Frt\text{-}G12D/+}$;*Ptf1a*$^{FlpO/+}$;*Lyz2*$^{Cre/+}$;*Arg1*$^{f/f}$ (KFCA) mouse model for the deletion of *Arg1* in myeloid cells during PDA tumorigenesis. Data shown here from mice aged 9–16 mo, n=24–26/group. (**E**) Representative hematoxylin and eosin (H&E) staining from age matching KF and KFCA mice. Scale bar, 100 μm. Histopathology evaluation shown on the right (n=26 KF and 24 KFCA, age matched, 9–16 mo old). Statistical significance was determined using chi-square test. Statistically significant when $P<0.05$. (**F**) Representative image of co-immunofluorescence staining for ARG1 (red), macrophages (F4/80, green), epithelial (CK19, gray), and DAPI (blue) in KF and KFCA tissue. Scale bar, 50 μm. Quantification on the right, n=5–6/group. Significance was determined using unpaired t test with Welch's correction. Statistically significant when $p<0.05$. (**G**) Uniform manifold approximation and projection (UMAP) visualization for the identified cell populations in merged KF and KFCA single-cell RNA sequencing. (**H**) Heatmap of top differentially expressed genes in the macrophage subclusters identified from KF and KFCA pancreata. (**I**) Dot plot visualization of *Arg1* and *Arg2* expression in KF and KFCA macrophage clusters. Average expression is shown by color intensity and expression frequency by dot size. (**J**) Reactome pathway enrichment analysis showing significantly upregulated pathways in KFCA macrophages.

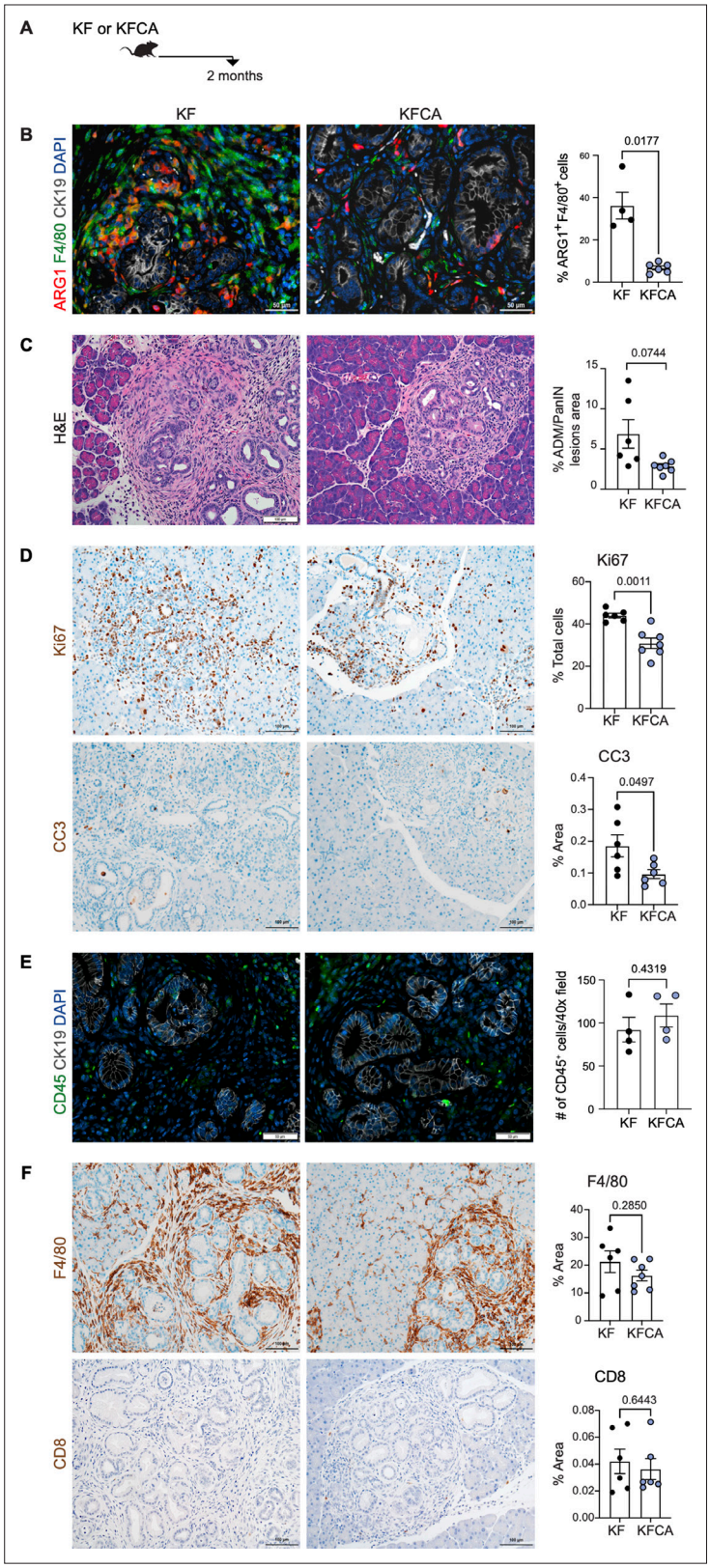

Figure 2—figure supplement 1. Deletion of Arginase 1 (*Arg1*) in myeloid cells decreases cell proliferation and cell death during early stages of pancreatic ductal adenocarcinoma. (**A**) Experimental design for KF and KFCA mice aged to 2 mo. (**B**) Representative images of co-immunofluorescence staining for ARG1 (red), macrophages (F4/80, green), epithelial (CK19, gray), and DAPI (blue) in KF and KFCA pancreata at 2 mo. Yellow staining shows

Figure 2—figure supplement 1 continued on next page

Figure 2—figure supplement 1 continued

co-localization of ARG1 and F4/80. Scale bar, 50 μm. Quantification on the right, n=4–6/group (**C**) Representative hematoxylin and eosin (H&E) images for KF and KFCA mice at 2 mo, n=6–7/group. Scale bar, 100 μm. On the right, percentage of ADM/PanIN lesions area in KF and KFCA tissue at 2 mo, n=6–7/group. (**D**) Representative immunohistochemistry staining for total cell proliferation (Ki67) and total cell death (cleaved caspase-3 [CC3]). Scale bar, 100 μm. Quantification on the right, n=6–7/group. (**E**) Representative immunofluorescence staining for immune cells (CD45, green) and epithelial cells (CK19, gray). Scale bar, 50 μm. Quantification on the right, n=4/group. (**F**) Representative immunohistochemistry staining for macrophages (F4/80) and $CD8^+$ T cells (CD8) in KF and KFCA tissue at 2 mo. Scale bar, 100 μm. Positive staining quantification is shown on the right. Student's t test was used to determine significance. Statistically significant when $p<0.005$.

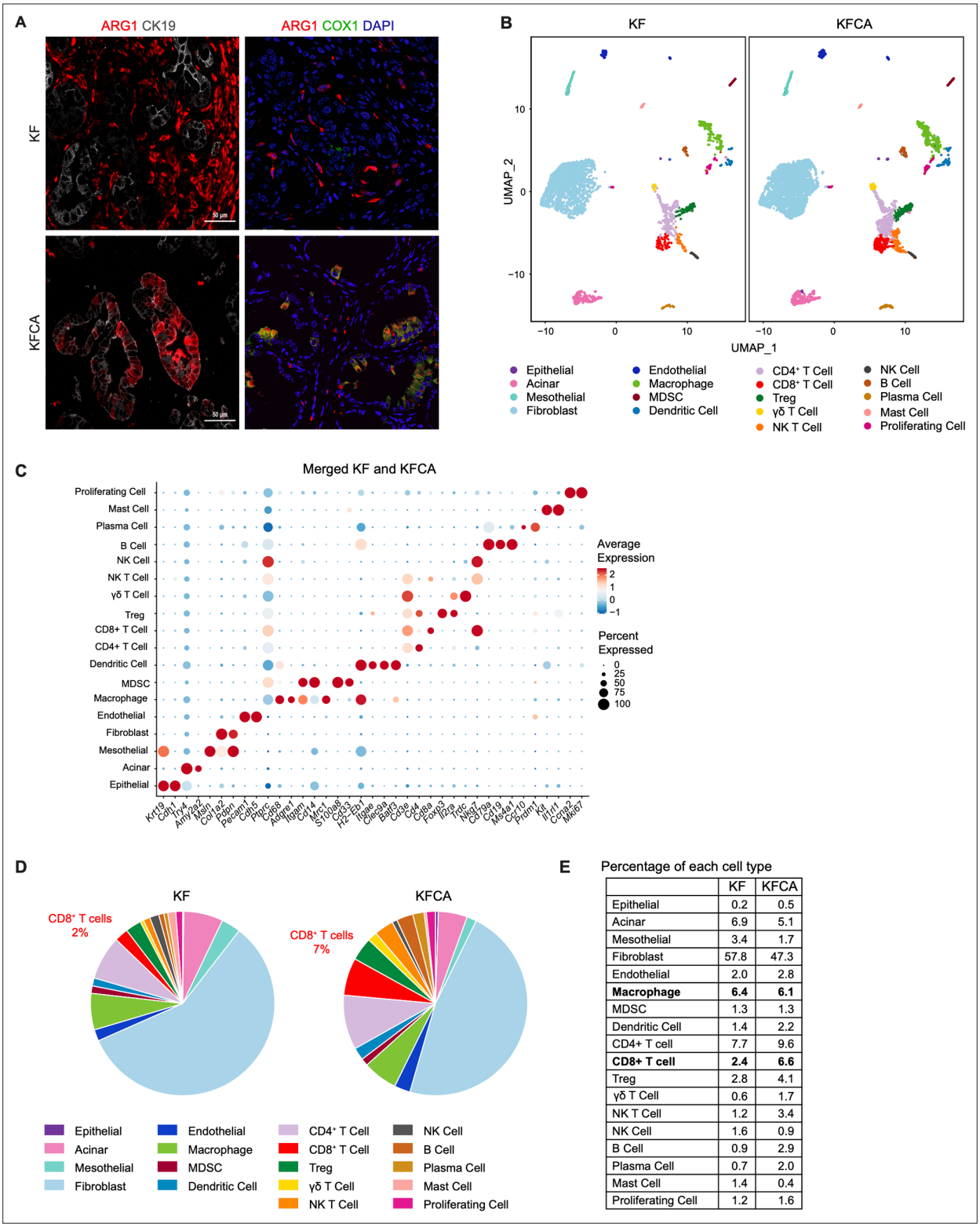

	KF	KFCA
Epithelial	0.2	0.5
Acinar	6.9	5.1
Mesothelial	3.4	1.7
Fibroblast	57.8	47.3
Endothelial	2.0	2.8
Macrophage	**6.4**	**6.1**
MDSC	1.3	1.3
Dendritic Cell	1.4	2.2
CD4+ T cell	7.7	9.6
CD8+ T cell	**2.4**	**6.6**
Treg	2.8	4.1
γδ T Cell	0.6	1.7
NK T Cell	1.2	3.4
NK Cell	1.6	0.9
B Cell	0.9	2.9
Plasma Cell	0.7	2.0
Mast Cell	1.4	0.4
Proliferating Cell	1.2	1.6

Figure 2—figure supplement 2. Deletion of Arginase 1 (*Arg1*) in myeloid cells alters the immune cell infiltration in a spontaneous pancreatic ductal adenocarcinoma mouse model during late stages of disease. (**A**) Left panel: co-immunofluorescence staining from ***Figure 2F*** showing ARG1 (*red*) and CK19 (gray) staining without DAPI; right panel: co-immunofluorescence staining for ARG1 (*red*), COX1 (*green*), and DAPI (*blue*) in KF and KFCA tissue. Scale bar, 50 μm. (**B**) Uniform manifold approximation and projection (UMAP) visualizations of single-cell RNA sequencing (sc-RNA-seq) comparing the identified cell populations in KF and KFCA. (**C**) Dot plot showing the lineage markers used to identify the distinct cell populations. Dot color indicates average expression, and dot size indicates expression frequency. (**D**) Pie charts comparing the proportion of the identified sc-RNA-seq populations between KF and KFCA. (**E**) Table showing the percentage of each identified population from total cells in KF and KFCA.

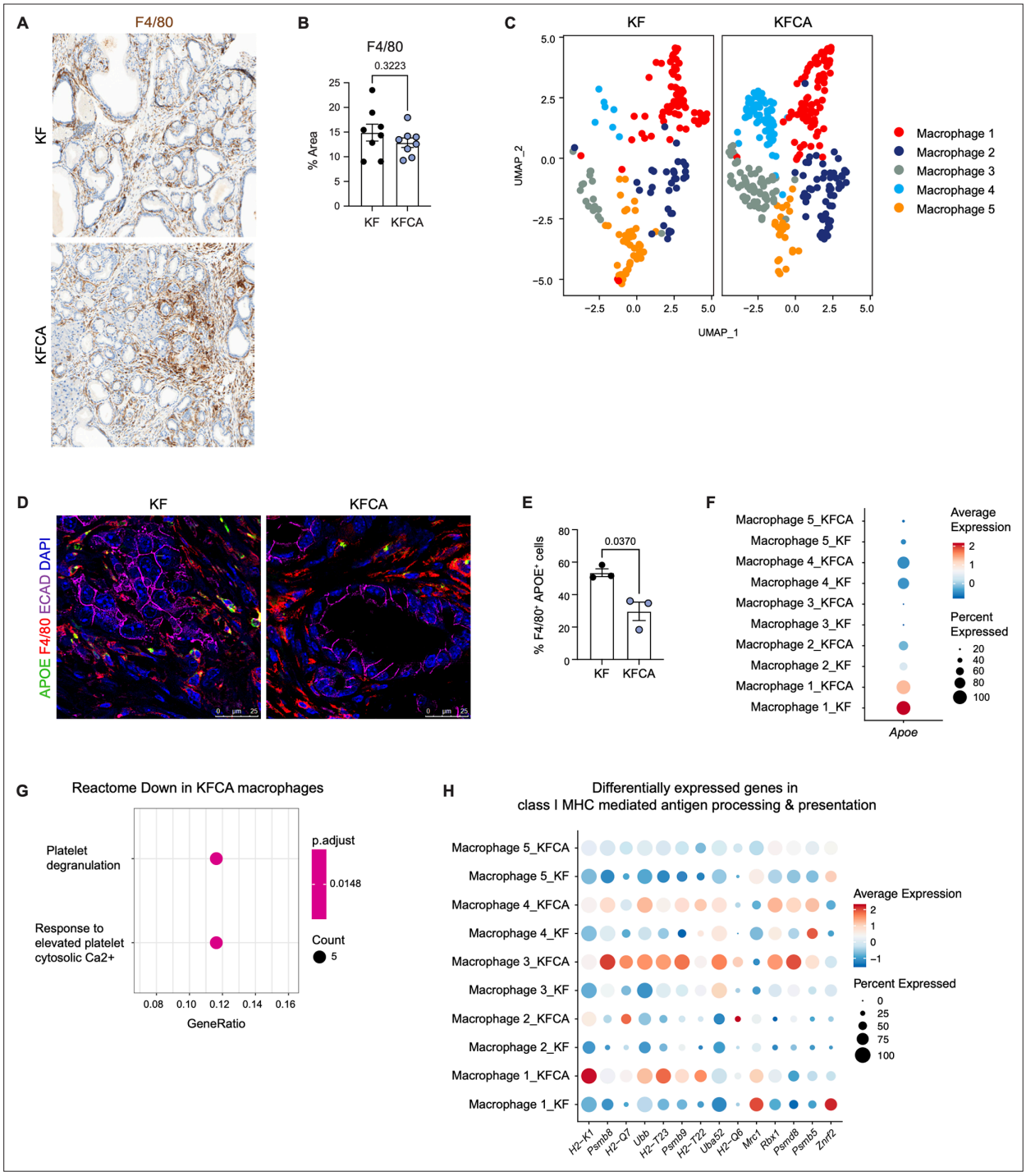

Figure 2—figure supplement 3. Deletion of Arginase 1 in myeloid cells decreases immune suppression in a spontaneous pancreatic ductal adenocarcinoma mouse model during late stages of the disease. (**A**) Representative immunohistochemistry staining for macrophages (F4/80) in KF and KFCA tissue during late stage of disease at 20× magnification. (**B**) Quantification for F4/80$^+$ staining, n=8/group. Student's t test was used to determine significance. (**C**) Uniform manifold approximation and projection (UMAP) visualizations showing the distribution of the five identified macrophage subpopulations in KF and KFCA. (**D**) Representative immunofluorescence staining for APOE (green), F4/80 (red), E-cadherin (ECAD; purple), and DAPI (blue) in KF and KFCA pancreas tissue during late stages of the disease. Scale bar, 25 μm. (**E**) Quantification of F4/80$^+$ APOE$^+$ cells, n=3/group. Student's t test was used to determine significance. (**F**) Dot plot visualization of *Apoe* expression in KF and KFCA macrophage clusters. Average expression is shown by color intensity, and percent expressed by dot size. (**G**) Reactome pathway enrichment analysis showing significantly downregulated pathways in KFCA macrophages. (**H**) Dot plot showing differentially expressed genes involved in MHC I-mediated antigen processing and presentation in macrophages.

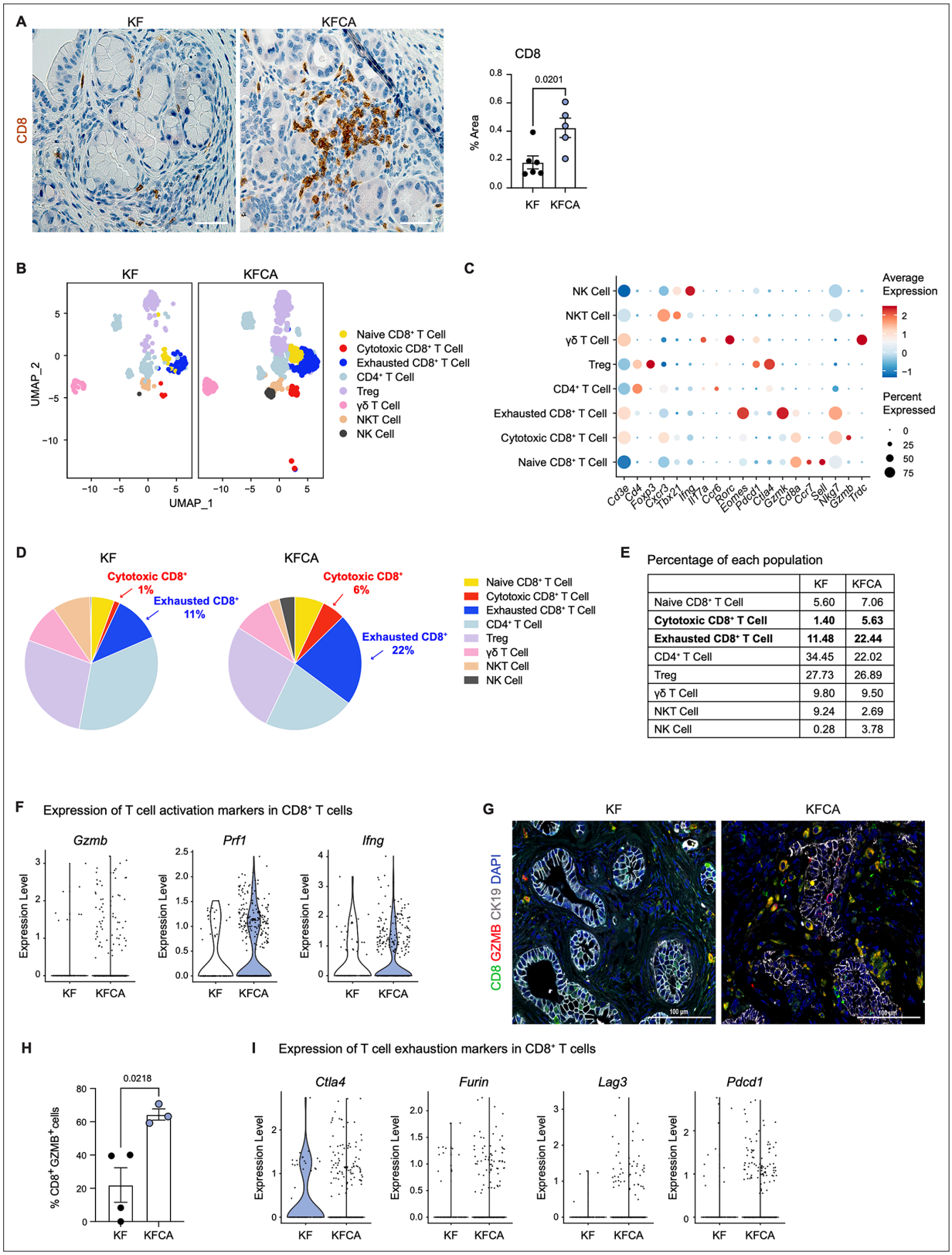

	KF	KFCA
Naive CD8⁺ T Cell	5.60	7.06
Cytotoxic CD8⁺ T Cell	**1.40**	**5.63**
Exhausted CD8⁺ T Cell	**11.48**	**22.44**
CD4⁺ T Cell	34.45	22.02
Treg	27.73	26.89
γδ T Cell	9.80	9.50
NKT Cell	9.24	2.69
NK Cell	0.28	3.78

Figure 3. Arginase 1 deletion in myeloid cells increases CD8⁺ T cell infiltration and activation in a spontaneous pancreatic ductal adenocarcinoma mouse model. (**A**) Representative images of CD8 immunohistochemistry staining (brown) in KF and KFCA tissue. Scale bar, 50 μm. Quantification of positive area on the right, n=5–6/group. Student's t test was used to determine statistical significance. (**B**) Uniform manifold approximation and projection (UMAP) visualization of defined T and natural killer (NK) cell clusters comparing single-cell RNA sequencing (sc-RNA-seq) data from KF and

Figure 3 continued on next page

Figure 3 continued

KFCA. (**C**) Dot plot of lineage markers used to identify the different types of lymphocytes. Dot size shows expression frequency, dot color shows average expression. (**D**) Pie charts showing the proportion of the identified lymphocyte populations in KF and KFCA sc-RNA-seq, percentage values are provided for populations that differ dramatically between KF and KFCA. (**E**) Table showing the percentage of each identified lymphocyte population in KF and KFCA sc-RNA-seq. (**F**) Violin plots showing normalized expression levels of T cell activation markers in all $CD8^+$ T cell populations identified in KF and KFCA sc-RNA-seq data. (**G**) Representative images of co-immunofluorescence staining for CD8 (green), GZMB (red), CK19 (gray), and DAPI (blue). Scale bar, 100 μm. (**H**) Quantification of $CD8^+$ $GZMB^+$ cells, n=3/group. Student's t test was used to determine significance. (**I**) Violin plots showing normalized expression levels of T cell exhaustion markers in all $CD8^+$ T cell populations identified in KF and KFCA.

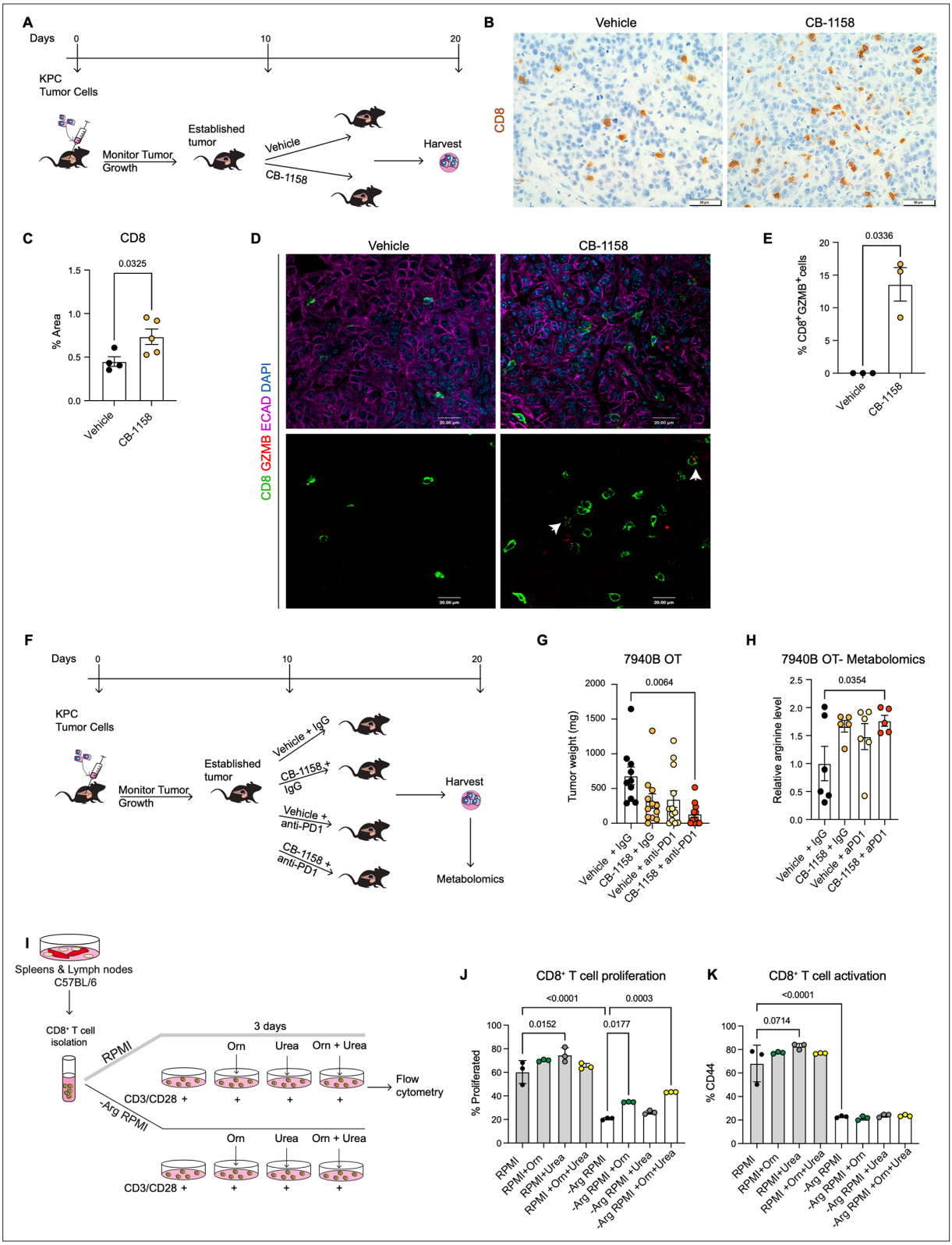

Figure 4. Systemic inhibition of arginase by CB-1158 in combination with anti-PD1 reduces tumor growth in an orthotopic pancreatic ductal adenocarcinoma mouse model. (**A**) Experimental timeline and design for orthotopic transplantation of 7940B KPC cells in syngeneic mice. (**B**) Representative images of immunohistochemistry staining for CD8 (brown). Scale bar, 50 μm. (**C**) Quantification of positive area of CD8 staining from B. Statistical significance was determined using unpaired t-test with Welch's correction. (**D**) Representative images of co-immunofluorescence staining for CD8 (green), GZMB (red), ECAD (purple), and DAPI (blue) in the vehicle and CB-1158 treated group. Scale bar, 20 μm. White arrows point to co-

Figure 4 continued on next page

Figure 4 continued

localization of CD8 (green) with GZMB (red). (**E**) Percentage of $CD8^+$ and $GZMB^+$ cells. Statistical significance was determined using unpaired t-test with Welch's correction. (**F**) Experimental timeline and design for orthotopic transplantation of 7940B KPC cells in syngeneic mice and different treatment groups. (**G**) Final tumor weight (mg) from the different treatment groups, n=10–12/group. Statistical significance was determined using two-way ANOVA with Tukey's multiple comparisons correction test. (**H**) Metabolomic analysis showing relative arginine levels in the tumors of the different treatment groups. Two-way ANOVA was used to determine statistical significance, n=5–6/group. (**I**) Experimental scheme for $CD8^+$ T cell isolation and growth in different media conditions. −Arg RPMI = RPMI lacking arginine, Orn = ornithine. (**J**) Percent of proliferated $CD8^+$ T cells from flow cytometry analysis. (**K**) Percent of activated $CD8^+$ T cells (CD44) from flow cytometry analysis. Two-way ANOVA with Tukey's multiple comparisons correction test was used to determine significance. n=3/condition.

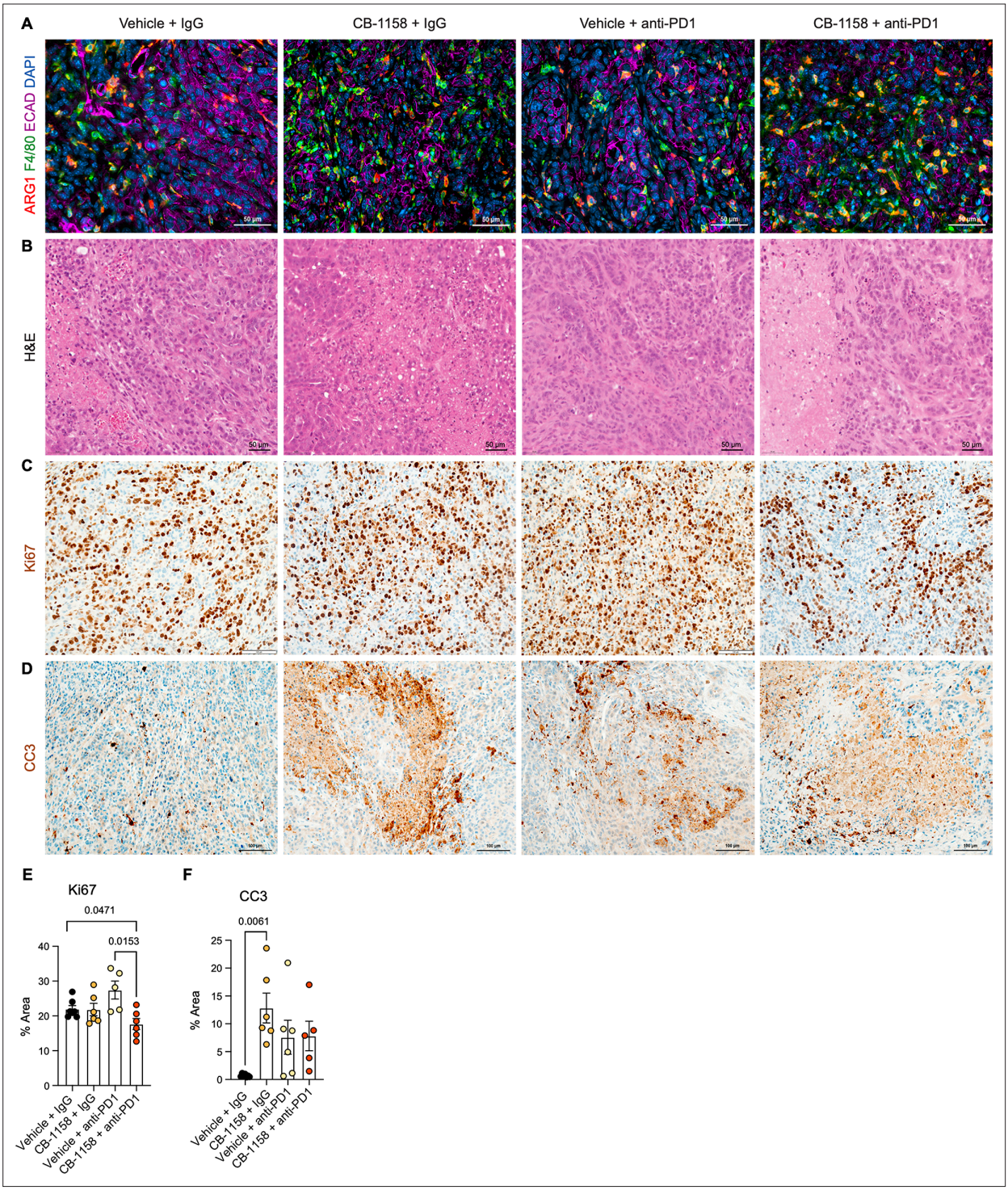

Figure 4—figure supplement 1. Histological analysis of the multiple treatment groups in the orthotopic mouse model. (**A**) Representative images of co-immunofluorescence staining for ARG1 (red), F4/80 (green), ECAD (purple), and DAPI (blue). Yellow shows co-localization of ARG1 with F4/80 macrophages. Scale bar, 50 μm. (**B**) Hematoxylin and eosin (H&E) staining for the indicated treatment groups. Scale bar, 50 μm. (**C**) Immunohistochemistry staining for cell proliferation (Ki67). Positive staining is shown in brown. Scale bar, 100 μm. (**D**) Immunohistochemistry staining for cell death (cleaved caspase-3 [CC3]). Positive staining is shown in brown. Scale bar, 100 μm. (**E and F**) Quantification of the positive staining area for Ki67 and CC3 from C and D. Significance was determined using unpaired t test with Welch's correction.

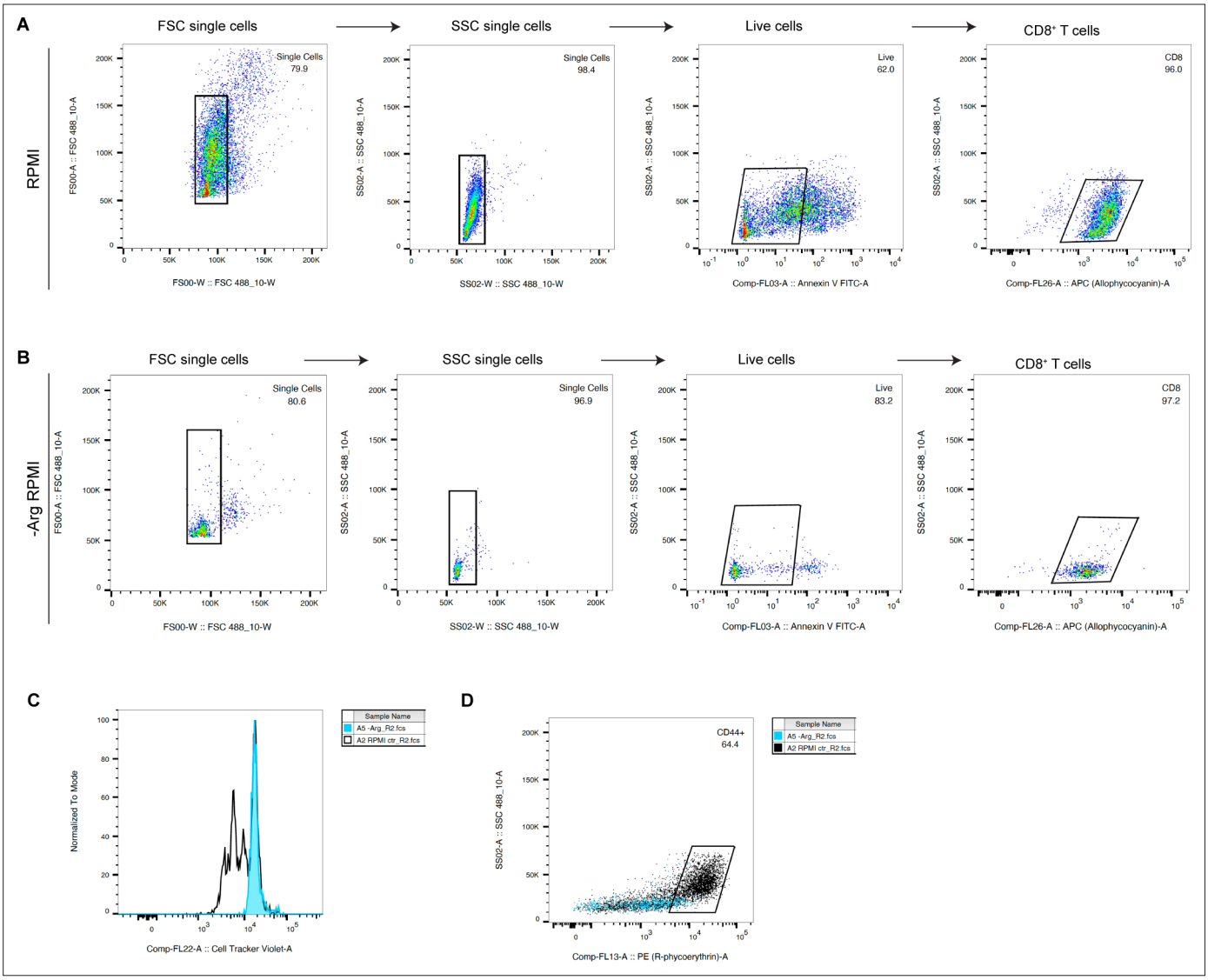

Figure 4—figure supplement 2. Flow cytometry gating strategy for CD8⁺ T cell proliferation and activation. (**A**) Representative gating strategy for cells cultured in RPMI control media. (**B**) Representative grating strategy for cells cultured in RPMI media lacking arginine (−Arg RPMI). (**C**) Proliferating lymphocytes. (**D**) Activated lymphocytes (CD44⁺).

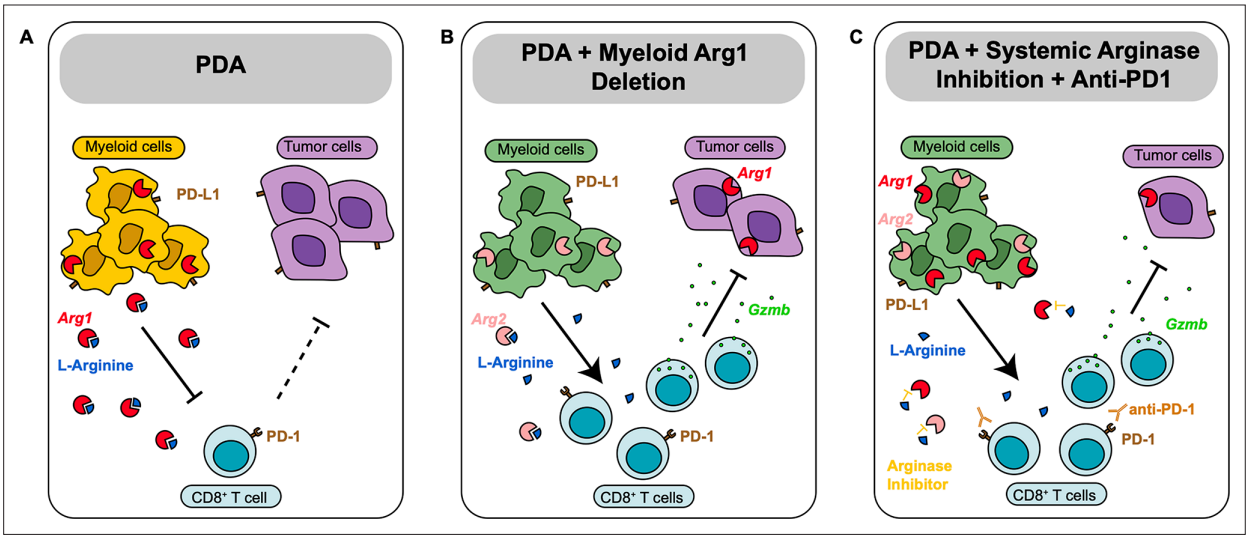

Figure 5. Diagram depicting our working model. (**A**) In pancreatic ductal adenocarcinoma (PDA), expression of *Arg1* in myeloid cells is immune suppressive. (**B**) Deletion of *Arg1* in myeloid cells in a spontaneous PDA mouse model induces macrophage repolarization and decreases tumor formation. (**C**) Systemic Arginase inhibition in combination with anti-PD1 immune checkpoint blockade further decreases tumor growth.